

Corrosion behaviour of β -Ti20Mo alloy in artificial saliva

Daniel Mareci · Romeu Chelariu · Ioan Dan ·
Doina-Margareta Gordin · Thierry Gloriant

Received: 1 October 2009 / Accepted: 3 August 2010 / Published online: 15 August 2010
© Springer Science+Business Media, LLC 2010

Abstract To evaluate the potential of β -Ti20Mo alloy as a dental material, we tested its corrosion behaviour in artificial saliva in comparison to that of cp-Ti. Open-circuit potential (E_{OC}), potentiodynamic polarization and electrochemical impedance spectroscopy (EIS) were used as electrochemical methods to characterize the corrosion behaviour of Ti20Mo alloy and cp-Ti, respectively. Corrosion current and passive current densities obtained from the polarization curves showed low values indicating a typical passive behaviour for Ti20Mo alloy. The EIS technique enabled us to study the nature of the passive film formed on the binary Ti20Mo alloy at various imposed potentials. The Bode phase spectra obtained for Ti20Mo alloy in artificial saliva exhibited two-time constants at higher potential (0.5 V, 1.0 V), indicating a two-layer structure. According to our experimental measurements, Ti20Mo alloy appears to possess superior corrosion resistance to that of cp-Ti in artificial saliva.

1 Introduction

Titanium and titanium alloys are widely used for structural biomedical and dental applications due to their low density, excellent biocompatibility, corrosion resistance and suitable mechanical properties [1–10].

A stable, adherent, compact and passive layer, consisting mainly of TiO_2 oxide, forms naturally on the surface of titanium and its alloys. This titanium oxide, an n-type semiconductor, has only ionic conductivity, and it is responsible for the high corrosion resistance of titanium and its alloys in various electrochemical media [11–13]. Thus, this oxide layer has an important role in terms of the biocompatibility of titanium-based biomaterials [14].

Due to its poor mechanical properties, cp-Ti is inadequate for most biomedical and dental applications so that it became necessary to use its alloys for such applications. Titanium alloys containing aluminium and vanadium elements exhibit higher strength than cp-Ti [15]. For this reason, Ti6Al4V alloy composition was the first titanium alloy used as implant material [16]. Further studies have indicated that vanadium, used to stabilize the β -phase, produces harmful oxides for the human body [17, 18]. The toxicity of vanadium pushed forward the development of new Ti-based alloys designed to replace Ti6Al4V. Khan et al. suggested [19] that Ti6Al7Nb could be a better alternative to Ti6Al4V due to its better corrosion resistance and stability in simulated body fluid environment with different pH values. Moreover, there have been concerns, not yet confirmed, about the connection between Al and Alzheimer disease [19, 20].

Nb, Ta, Zr, Mo and Sn have been selected as safe alloying elements to titanium, since they are judged as non-toxic and non-allergic [21]. In addition, alloying titanium with isomorphous β -stabilizers such as Mo, Nb and Ta is known to improve the mechanical properties [22, 23].

D. Mareci
Gheorghe Asachi Technical University of Iasi,
Faculty of Chemical Engineering and Environmental Protection,
71A D. Mangeron Blvd., 700050 Iasi, Romania

R. Chelariu (✉)
Gheorghe Asachi Technical University of Iasi,
Faculty of Materials Science and Engineering,
61A D. Mangeron Blvd., 700050 Iasi, Romania
e-mail: rchelariu@yahoo.com

I. Dan
R&D Consultanta si Servicii,
45 Maria Ghiculeasa Str., 023761 Bucharest, Romania

D.-M. Gordin · T. Gloriant
INSA Rennes, UMR CNRS 6226 Sciences Chimiques de
Rennes/Chimie-Métallurgie 20 avenue des Buttes de Coesmes,
35043 Rennes Cedex, France

Therefore, new V and Al free binary alloys, having non-toxic elements, such as Ti45Nb [24], Ti35Nb [25], TiHf [26], TiTa [27], TiMo [28–32] have been developed in the last decades. Due to its high β -stabilizer power, the Mo element was recently used as alloying element and different compositions, such as Ti15Mo (%wt.) [28], Ti10Mo (%wt.) [29], Ti(4 ÷ 20)Mo (%wt.) [30, 31], Ti(5 ÷ 35)Mo (%wt.) [33], were investigated in view of their biomedical and dental applications.

In the pre-clinical testing of the metallic biomaterials used in dental applications, the in vitro corrosion behaviour tests in different artificial saliva media have a well-defined importance. Human saliva can vary to a considerable degree and is dependent on the age and sex of the patient, the time of day, eating habits, medication and oral hygiene [34]. In this study, we selected Fusayama's artificial saliva because the results obtained with this medium are consistent with the clinical experience of dental alloys [35].

The corrosion behaviour of β -Ti20Mo (%wt.) alloy in Fusayama's artificial saliva has been investigated in comparison to commercial pure titanium (cp-Ti) using potential-time measurements, potentiodynamic polarization and EIS measurements.

2 Materials and methods

2.1 Materials

Cold crucible levitation melting (CCLM) (Metallurgical Chemistry Laboratory, INSA Rennes, France) in a high frequency induction furnace under a pure argon atmosphere stabilized after several cycles of argon charging-high vacuum pumping, was the technique used to synthesize small ingots of Ti20Mo alloy. In order to eliminate segregation, the Ti20Mo alloy ingots were homogenized by heat treatment performed in a tubular furnace under high-vacuum ($10^{-7} \div 10^{-6}$ mbar) using the following conditions: (1) heating from room temperature at $5^\circ\text{C}/\text{min}$, (2) homogenization at a β -transus temperature + 100°C for 24 h and (3) natural cooling. The synthesis and structural characterization of the β -type Ti alloys containing Mo as β -stabilizer element were detailed elsewhere [36]. The cp-Ti samples were made from a bar stock in annealed state (delivered by R&D Consultanta si Servicii SRL, Bucharest, Romania).

2.2 Corrosion tests

2.2.1 Corrosion medium

Fresh Fusayama's artificial saliva [37] used as corrosion medium, was prepared before use. It is composed of 0.400 g NaCl; 0.400 g KCl; 0.795 g $\text{CaCl}_2 \cdot 2\text{H}_2\text{O}$; 0.780 g

$\text{NaH}_2\text{PO}_4 \cdot 2\text{H}_2\text{O}$; 0.005 g $\text{Na}_2\text{S} \cdot 9\text{H}_2\text{O}$; 1.000 g NH_2CONH_2 and distilled water up to 1000 mL. The solution has a pH value of about 5.6. Because the short-term pH variations of human saliva include the intake of acidic beverages (pH 2–3) and secretion of gastric acid (pH 1), we added lactic acid to Fusayama's artificial saliva to decrease the pH value to 2.5 in order to accentuate the corrosion.

2.2.2 Corrosion setup

Electrochemical measurements were carried out in aerated artificial saliva at 25°C using a Princeton Applied Research potentiostat (Model 263 A) connected to a Princeton Applied Research 5210 lock-in amplifier. The electrochemical system was controlled by a personal computer with a specific software package called Electrochemistry Power Suite (Princeton Applied Research).

All the electrochemical measurements were performed using a conventional three-electrode system. Working electrodes made from both the Ti20Mo alloy and cp-Ti samples and a platinum sheet as counter electrode and a saturated calomel electrode (SCE) as reference electrode were used. All potentials are referred to SCE in this article. The working electrode was prepared by attaching a brass nut to one side of the specimen with conductive resin. Moreover, the preparation of the samples made it possible to leave a surface of 0.2 cm^2 free. Each surface was polished with emery sheets (from 600 to 2000 grit) and was then mirror-polished by means of $1 \mu\text{m}$ alumina aqueous solution. Afterwards, each surface was cleaned using methanol and distilled water.

2.2.3 Open-circuit potential

The open-circuit potential (E_{OC}) measurement of each specimen was first recorded for 24 h after immersion in each electrolyte. This period seemed sufficient to attain steady-state conditions.

2.2.4 Potentiodynamic polarization

The potentiodynamic polarization curve was recorded by means of a potential scanning rate of $0.5 \times 10^{-3} \text{ V/s}$ from -0.8 V to $+1.5 \text{ V}$, and reversed in the negative direction to $+1.0 \text{ V}$. We used the automatic data acquisition system to plot the potentiodynamic polarization curves. Both the anodic and cathodic branches of the Tafel plots were useful to estimate the corrosion rate and potential.

2.2.5 Electrochemical impedance spectroscopy

Aerated artificial saliva (25°C) subjected to the following different potentials: -0.5 V (approaching the ZCP value for

both titanium-based materials), 0.0 V, 0.5 V and 1.0 V, was used to perform EIS measurements. The EIS results were recorded in the 10^{-2} – 10^5 Hz frequency range. The over potential was applied after 30 min. The amplitude of the alternative potential applied was 10^{-2} V.

In order to supply quantitative support for discussions on these experimental EIS results, an appropriate model (ZSimpWin-PAR, USA) for equivalent circuit (EC) quantification was used.

3 Results and discussion

3.1 Open-circuit potential

Figure 1 shows the open-circuit potential (E_{OC}) versus time behaviour of Ti20Mo alloy and cp-Ti in artificial saliva.

After fresh surface polishing of Ti20Mo alloy and cp-Ti exposed to humid air, a thin oxide layer is spontaneously formed on their surfaces. After the samples' immersion into the electrolyte, the open circuit potential increases rapidly with time. As concerns Ti20Mo alloy, the initial open circuit potential is around -0.600 V and after approximately 1 h of immersion, this value rises to about -0.400 V. This initial E_{OC} increase seems to be related to the thickening of the oxide film, which improves its corrosion protection ability [7]. Afterwards, the E_{OC} value increases slowly suggesting the growth of the film onto the metallic surface [10]. The potential was stable from 10 h onwards. The samples from cp-Ti have a similar behaviour. However, cp-Ti shows nobler potential than Ti20Mo alloy probably due to the formation of a pure TiO_2 oxide film, as compared to the mixed oxide formation on Ti20Mo alloy possibly consisting of TiO_2 and Mo_2O_5 [31]. The samples

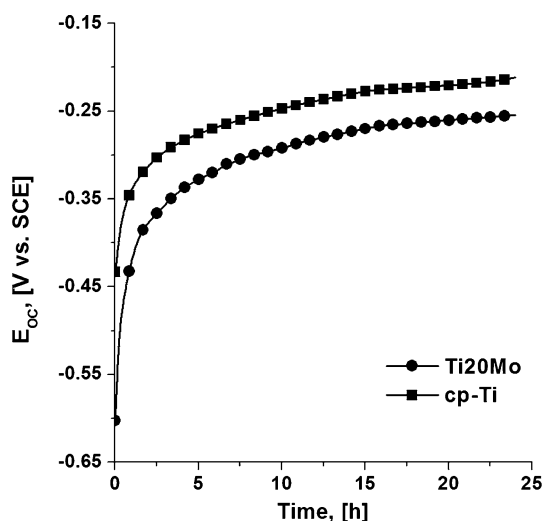


Fig. 1 The open circuit potential (E_{OC}) versus time for Ti20Mo alloy and cp-Ti in artificial saliva

of both titanium-based materials did not exhibit potential drops associated with surface activation during the 24 h exposure in artificial saliva. This kind of behaviour suggests that the air-formed native oxide is kinetically resistant to chemical dissolution in artificial saliva.

3.2 Potentiodynamic polarization

Figure 2 shows the polarization curves of Ti20Mo alloy and cp-Ti in artificial saliva. Prior to polarization measurement, the electrode was cathodically polarized at -1.5 V in the working solution for 60 s in order to remove any spontaneously formed surface film [11].

PowerCorr software (PAR, USA) was used to extract the zero current potential (ZCP) and corrosion current density (J_{corr}) values from the potentiodynamic polarization plot. Both samples reach their respective stable passive current densities as the potential increases. Passive current density (J_{pass}) was also determined from the potentiodynamic anodic diagram at different potentials (0.0, 0.5 and 1.0 V). The ZCP, J_{corr} and J_{pass} values from two different polarization curves are shown in Table 1. Figure 2 clearly proves that Ti20Mo alloy possesses a corrosion resistance superior

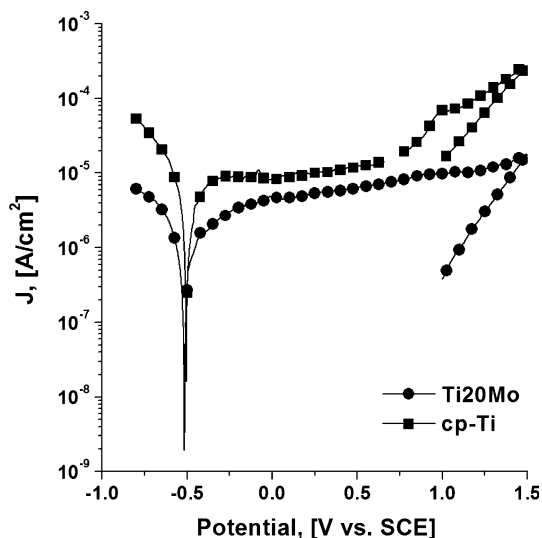


Fig. 2 Potentiodynamic polarization curve recorded over the range of -0.8 V to 1.5 V and reverse to 1.0 V for Ti20Mo alloy and cp-Ti in artificial saliva, at 25°C and $dE/dt = 0.5 \times 10^{-3} \text{ Vs}^{-1}$

Table 1 The main parameters of the corrosion process measured for the Ti20Mo alloy and cp-Ti in artificial saliva at 25°C

Samples	ZCP [V]	J_{corr} [$\mu\text{A}/\text{cm}^2$]	J_{pass} [$\mu\text{A}/\text{cm}^2$]		
			0.0 V	0.5 V	1.0 V
Ti20Mo	-0.517	0.6	4.8	6.3	8.9
cp-Ti	-0.504	2.2	8.1	13.2	79.4

to that of cp-Ti in artificial saliva. As for Ti20Mo alloy, the passive current density is nearly stable when the potential increases from 0.0 V to 1.0 V.

The current exhibited a negative hysteresis when the scan was reversed and no pits were found on the samples after the polarization test.

Passive current densities (J_{pass}) are higher than corrosion current densities (J_{corr}) suggesting that the protective Ti oxide film can be more defective [7, 15]. The lower corrosion current densities and the lower and more stable passive current densities of Ti20Mo alloy indicate that Ti20Mo alloy possesses a better corrosion resistance than the cp-Ti in artificial saliva.

3.3 Electrochemical impedance spectroscopy

EIS data contain information on the passive film characteristics. The fitting quality of EIS data was estimated by both the chi-square (χ^2) test (between 10^{-5} and 10^{-4}) values and the comparison between error distribution versus frequency values ($\pm 2\%$ for the whole frequency range) corresponding to experimental and simulated data. The chi-square (χ^2) and error distribution versus frequency values point to the excellent agreement between the experimental and simulated values.

The impedance spectroscopy results for Ti20Mo alloy and cp-Ti in artificial saliva at different selected potentials are shown in the Bode diagrams in Figs. 3, 4, 5, and 6. The phase angle maxima noticed for Ti20Mo alloy and cp-Ti lie in the range of approximately -70° to -80° . The phase angle values, between -70° and -80° in a large frequency range (0.1 ÷ 100 Hz) both for cp-Ti (-0.5 V) and Ti20Mo

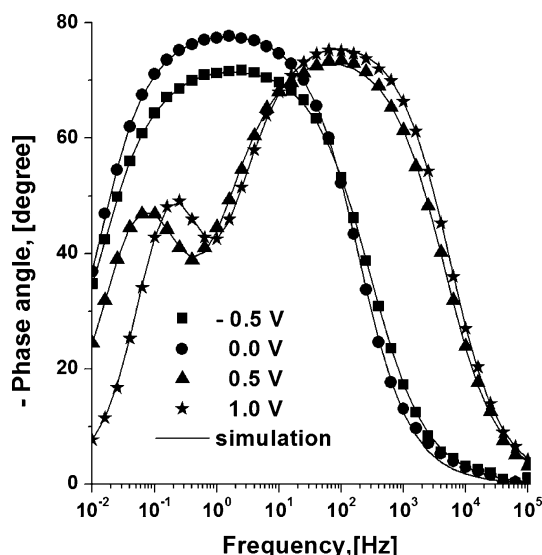


Fig. 3 Phase angle Bode spectra for Ti20Mo alloy tested at different potentials in artificial saliva at 25°C

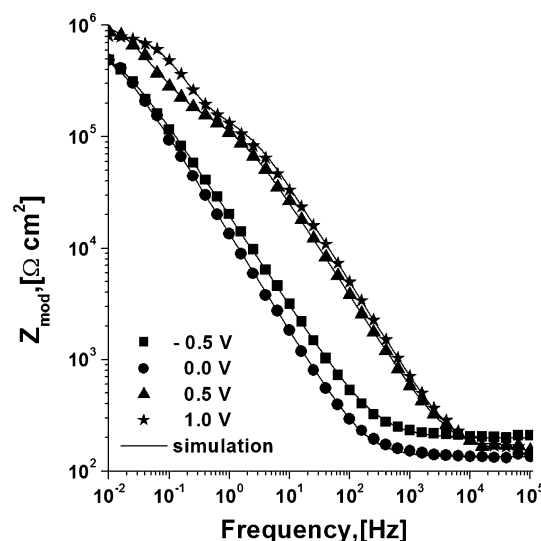


Fig. 4 Z Bode spectra for Ti20Mo alloy tested at different potentials in artificial saliva at 25°C

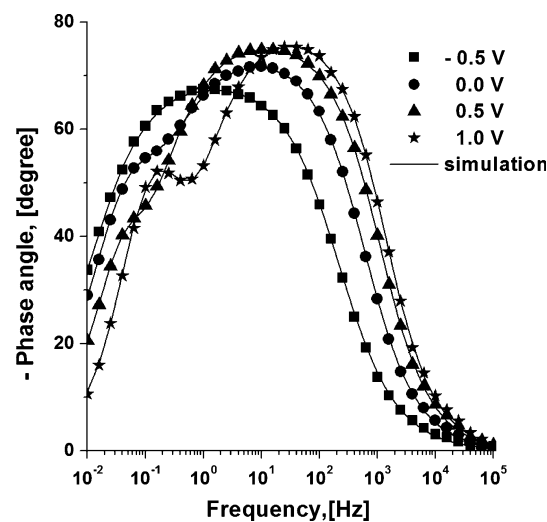


Fig. 5 Phase angle Bode spectra for cp-Ti tested at different potentials in artificial saliva at 25°C

alloy (-0.5 V and 0.0 V), are characteristic values of a compact passive film [4]. The high impedance values ($10^5 \Omega \text{ cm}^2$ order) obtained from medium to low frequencies for these samples suggest a high corrosion resistance in artificial saliva.

The phase angle plots (Figs. 3 and 5) reveal only one peak both for cp-Ti at -0.5 V and Ti20Mo alloy at -0.5 V and 0.0 V, indicating the involvement of a single time constant. This behaviour usually indicated that a thin passive oxide film was formed on the surface [38]. The results of the analysis are shown in Table 2. The simple equivalent circuit (EC) consisting of only one time constant (Fig. 7a) was used to model the experimental impedance spectra. A

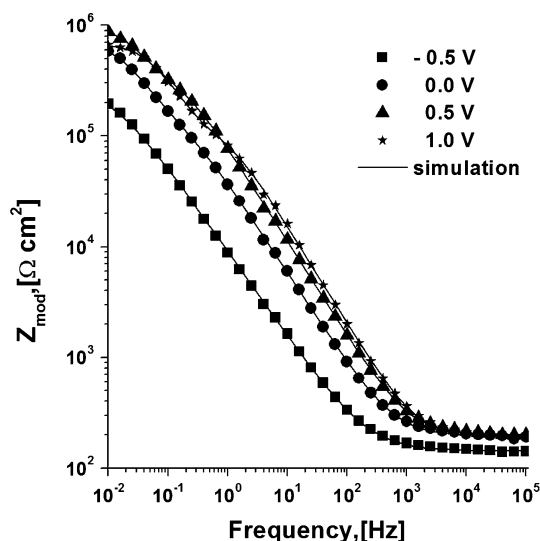


Fig. 6 Z Bode spectra for cp-Ti tested at different potentials in artificial saliva at 25°C

good agreement between the experimental data and fitted data was obtained. The R_{bL} and Q_{bL} parameters describe the processes occurring at the electrolyte/dense passive film interface. R_{sol} is the ohmic resistance of the electrolyte. The same R_{sol} value, that is $53 \pm 3 \Omega$, was noticed in all the cases. Studies performed on various Ti-based alloys under physiological conditions showed that this simple EC could be used successfully to describe the corrosion behaviour of titanium alloys [4, 8, 31, 39, 40].

The Q symbol reveals the possibility of a non-ideal capacitance (CPE, constant phase element). The CPE relies on the fact that, experimentally, the barrier film never exhibits the theoretically expected phase shift of -90° and a slope of -1 for an ideal dielectric. The following equation [41] calculates the CPE impedance:

$$Q = Z_{CPE} = \frac{1}{C(j\omega)^n} \tag{1}$$

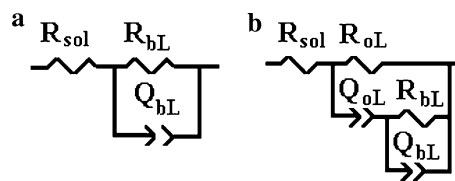


Fig. 7 Equivalent circuits (EC) used to fit the impedance data

where, when $n = 1$, the Q element is reduced to a capacitor with a capacitance C , and when $n = 0$, it is reduced to a simple resistor. This n is related to a slope of the Log (Z_{mod}) versus Log (Frequency) Bode-plots, ω is the angular frequency and j is an imaginary number ($j^2 = -1$).

The barrier layer resistance of Ti20Mo alloy at -0.5 V is about two times higher than that of cp-Ti. The $0.8 n_{bL}$ value indicates the deviation from a near capacitance behaviour of both titanium-based materials at -0.5 V and of Ti20Mo alloy at 0.0 V.

The impedance spectra fitting for Ti20Mo alloy at 0.5 V and 1.0 V and for cp-Ti at 0.0 V, 0.5 V and 1.0 V was carried out with an EC (Fig. 7b) using a series combination of the R_{sol} solution resistance, with two RQ elements in parallel: $R_{sol}(R_{oL}(Q_{oL}(R_{bL}Q_{bL})))$. Again, a very good agreement between the simulated and experimental data was obtained. The $R_{sol}(R_{bL}Q_{bL})$ model failed to provide a satisfactory fit (the values of the chi-square (χ^2) test were about 10^{-2}). Table 2 shows the results of the fittings.

This EC is based on a model used by Pan et al. [3] to simulate data in saline solution. These authors noticed that the surface layer formed on titanium is in fact a two-layer oxide: an inner barrier layer and an outer porous layer. Studies performed on Ti-based alloys under physiological conditions showed that the EC proposed by Pan et al. [3] successfully describes the behaviour of these materials as well [4, 7, 10, 13, 42]. The high-frequency R_{oL} and Q_{oL} parameters are the properties of the reactions at the outer porous passive film/solution interface. The R_{bL} and Q_{bL}

Table 2 Values of fitted parameters of the equivalent circuits as a function of applied potential of Ti20Mo alloy and cp-Ti in artificial saliva

Samples	Imposed potential [V]	EC model	Q_{oL} [$S\ cm^{-2}\ s^n$], $\times 10^6$	n_{oL}	R_{oL} [$k\Omega\ cm^2$]	Q_{bL} [$S\ cm^{-2}\ s^n$], $\times 10^6$	n_{bL}	R_{bL} [$k\Omega\ cm^2$]
Ti20Mo	-0.5 ($\approx ZCP$)	$R_{sol}(R_{bL}Q_{bL})$	–	–	–	14.8	0.81	641
	0.0		–	–	–	8.7	0.84	782
	0.5	$R_{sol}(R_{oL}(Q_{oL}(R_{bL}Q_{bL})))$	1.2	0.86	161	6.2	0.89	1120
	1.0		1.1	0.86	250	4.6	0.90	893
cp-Ti	-0.5 ($\approx ZCP$)	$R_{sol}(R_{bL}Q_{bL})$	–	–	–	34.1	0.80	342
	0.0	$R_{sol}(R_{oL}(Q_{oL}(R_{bL}Q_{bL})))$	5.5	0.83	132	11.0	0.83	549
	0.5		2.7	0.85	379	9.1	0.89	522
	1.0		1.9	0.87	281	7.9	0.91	521

parameters describe the processes occurring to the electrolyte/dense passive film interface.

High resistance values of the outer layer ($10^5 \Omega \text{ cm}^2$ order) were found for both samples. These values indicate the formation of a porous layer with a good corrosion resistance [7].

As for Ti20Mo alloy, barrier layer resistance increases as the potential increase from -0.5 V to 0.5 V , and then decreases slowly as the potential increases to 1.0 V . The resistance decrease indicates that the oxide layer may become more defective at high over potential [7, 15]. However, the R_{bL} of Ti20Mo alloy in artificial saliva was still high at 1.0 V as seen in Table 2. This indicates that the alloy is highly resistant to corrosion even at very high over potentials. As concerns cp-Ti, as potential increases from 0.0 V to 1.0 V , barrier layer resistance remains approximately constant (around $5 \times 10^5 \Omega \text{ cm}^2$), probably due to the fact that the titanium oxide is essentially TiO_2 [3]. The higher R_{bL} of Ti20Mo alloy for all the potentials indicates that this alloy possesses better corrosion resistance than cp-Ti in artificial saliva, supporting the results obtained from the polarization tests. For both samples, the R_{bL} (inner barrier layer) is about $2 \div 5$ times higher than the R_{oL} (porous layer). This reveals that the inner barrier layer provides most of the protection.

However, the R_{oL} value is high ($10^5 \Omega \text{ cm}^2$ order) for both samples. It may be possible that the lactic acid molecules were adsorbed on the sample surface during the polarization, which would explain the increase in the R_{oL} resistance.

Also, it is worthy to note that the n_{bL} values, corresponding to 0.5 V and at 1.0 V for both samples, were found to be around 0.9. This indicates that the film exhibits a near capacitive behaviour.

4 Conclusions

We showed that electrochemical techniques play an overwhelming role in evaluating corrosion resistance. Considering the electrochemical measurements, the following conclusions could be drawn:

1. A passive film was formed on Ti20Mo alloy during the corrosion tests carried out in Fusayama's artificial saliva. Its formation was accompanied by very low experimental current densities.
2. The Bode phase spectra recorded for Ti20Mo alloy in Fusayama's artificial saliva exhibited single-time constant at lower potential (-0.5 V , 0.0 V), indicating a single layer structure. Bode phase spectra for both samples showed two-time constant at higher potential (0.5 V , 1.0 V) and were fitted with an equivalent

circuit (EC) characterized by two RQ elements in parallel. This EC is consistent with the model of a two-layer structure for passive films: an inner barrier layer with high impedance, responsible for corrosion protection, and an outer porous layer. Ti20Mo alloy appears to possess superior corrosion resistance to that of cp-Ti in artificial saliva.

3. The corrosion parameters experimentally obtained for the Ti20Mo alloy in Fusayama's artificial saliva suggest that this material has dental use potential.

References

1. Williams DF. Biocompatibility of clinical implant materials. In: Williams DF, editor. Biocompatibility of clinical implant materials, vol.1. Boca Raton: CRC Press; 1981. p. 9–44.
2. Kovacs P, Davidson JA. Chemical and electrochemical aspects of the biocompatibility of titanium and its alloys. In: Brown SA, Lemons JE, editors. Medical applications of titanium and its alloys: the materials and biological issues. ASTM STP 1272. West Conshohocken: ASTM; 1996. p. 163–78.
3. Pan J, Thierry D, Leygraf C. Electrochemical impedance spectroscopy study of the passive oxide film on titanium for implant application. *Electrochim Acta*. 1996;141:1143–53.
4. Gonzalez JEG, Mirza Rosca JC. Study of the corrosion behavior of titanium and some of its alloys for biomedical and dental implant applications. *J Electroanal Chem*. 1999;471:109–15.
5. Long MJ, Rack HJ. Titanium alloys in total joint replacement—a materials science perspective. *Biomaterials*. 1998;19:1621–39.
6. Kim HS, Lim SH, Yeo ID, Kim WY. Stress-induced martensitic transformation of metastable β -titanium alloy. *Mater Sci Eng A*. 2007;449–451:322–5.
7. Assis SL, Wolynec S, Costa I. Corrosion characterization of titanium alloys by electrochemical techniques. *Electrochim Acta*. 2006;51:1815–9.
8. Raman V, Nagarajan S, Rajendran N. Electrochemical impedance spectroscopic characterisation of passive film formed over β Ti–29Nb–13Ta–4.6 Zr alloy. *Electrochem Comm*. 2006;8:1309–14.
9. Lee TM. Effect of passivation and surface modification on the dissolution behavior and nano-surface characteristics of Ti-6Al-4 V in Hank/EDTA solution. *J Mater Sci Mater Med*. 2006;17: 15–27.
10. Mareci D, Ungureanu G, Aelenei D, Mirza Rosca JC. Electrochemical characteristics of titanium based biomaterials in artificial saliva. *Mater Corros*. 2007;11:848–56.
11. Metikos-Hukovic M, Kwokal A, Piljac J. The influence of niobium and vanadium on passivity of titanium-based implants in physiological solution. *Biomaterials*. 2003;24:3765–75.
12. Milosev I, Metikos-Hukovic M, Strehblow HH. Passive film on orthopaedic TiAlV alloy formed in physiological solution investigated by X-ray photoelectron spectroscopy. *Biomaterials*. 2000;21:2103–13.
13. Milosev I, Kosec T, Strehblow HH. XPS and EIS study of the passive film formed on orthopaedic Ti–6Al–7Nb alloy in Hank's physiological solution. *Electrochim Acta*. 2008;53:3547–58.
14. Elias CN, Oshida Y, Cavalcante Lima JH, Muller CA. Relationship between surface properties (roughness, wettability and morphology) of titanium and dental implant removal torque. *J Mech Behav Biomed Mater*. 2008;1:234–42.

15. Van Noort R. Titanium: the implant material of today. *J Mater Sci*. 1987;22:3801–11.
16. Niinomi M. Mechanical properties of biomedical titanium alloys. *Mater Sci Eng A*. 1998;243:231–6.
17. Kim TI, Han JH, Lee IS, Lee KH, Shin MC, Choi BB. New titanium alloys for biomaterials: a study of mechanical and corrosion properties and cytotoxicity. *Biomed Mater Eng*. 1997;7:253–63.
18. Khan MA, Williams RL, Williams DF. In vitro corrosion and wear of titanium alloys in the biological environment. *Biomaterials*. 1996;17:2117–26.
19. Okazaki Y, Ito Y, Kyo K, Tateishi T. Corrosion resistance and corrosion fatigue strength of new titanium alloys for medical implants without V and Al. *Mater Sci Eng A*. 1996;213:138–47.
20. Rao S, Okazaki Y, Tateishi T, Ushida T, Ito Y. Cytocompatibility of new Ti alloy without Al and V by evaluating the relative growth ratios of fibroblasts L929 and osteoblasts MC3T3–E1 cells. *Mater Sci Eng C*. 1997;4:311–4.
21. Niinomi M. Recent research and development in titanium alloys for biomedical applications and healthcare goods. *Sci Tech Adv Mater*. 2003;4:445–54.
22. He G, Eckert J, Dai QL, Sui ML, Loser W, Hagiwara M, Ma E. Nanostructured Ti-based multi-component alloys with potential for biomedical applications. *Biomaterials*. 2003;24:5115–20.
23. Ho WF, Ju CP, Chern Lin JH. Structure and properties of cast binary Ti–Mo alloys. *Biomaterials*. 1999;20:2115–22.
24. Godley R, Starosvetsky D, Gotman I. Corrosion behaviour of a low modulus β -Ti-45%Nb alloy for use in medical implants. *J Mater Sci Mater Med*. 2006;17:63–7.
25. Cremasco A, Osorio WR, Freire CMA, Garcia A, Caram R. Electrochemical corrosion behavior of a Ti-35Nb alloy for medical prostheses. *Electrochim Acta*. 2008;53:4867–74.
26. Cai Z, Koike M, Sato H, Brezner M, Guo Q, Komatsu M, Okuno O, Okabe T. Electrochemical characterization of cast Ti–Hf binary alloys. *Acta Biomater*. 2005;1:353–6.
27. Gordin DM, Delvat E, Chelariu R, Ungureanu G, Besse M, Laille D, Gloriant T. Characterization of Ti–Ta alloys synthesized by cold crucible levitation melting. *Adv Eng Mater*. 2008;10:714–9.
28. Niinomi M. Mechanical biocompatibilities of titanium alloys for biomedical applications. *J Mech Behav Biomed Mater*. 2008;1:30–42.
29. Alvez Rezende MCR, Rosifini Alvez AP, Codaro EN, Matsumoto Dutra CA. Effect of commercial mouthwashes on the corrosion resistance of Ti-10Mo experimental alloy. *J Mater Sci Mater Med*. 2007;18:149–54.
30. Oliveira NTC, Gustaldi AC. Electrochemical behaviour of Ti–Mo alloys applied as biomaterial. *Corros Sci*. 2008;50:938–45.
31. Oliveira NTC, Gustaldi AC. Electrochemical stability and corrosion resistance of Ti–Mo alloys for biomedical applications. *Acta Biomater*. 2009;5:399–405.
32. Kumar S, Sankara Narayanan TSN. Corrosion behaviour of Ti-15Mo alloy for dental implant applications. *J Dent*. 2008;36:500–7.
33. Bartáková S, Prachár P, Kudrman J, Březina V, Podhorná B, Černochová P, Vaněk J, Strecha J. New titanium β -alloys for dental implantology and their laboratory-based assays of biocompatibility. *Scr Medica*. 2009;82:76–82.
34. Holland RI. Corrosion testing by potentiodynamic polarization in various electrolytes. *Dent Mater*. 1992;8:241–5.
35. McCabe JF. *Applied dental materials*. 7th ed. Oxford: Blackwell Science; 1990.
36. Gloriant T, Texier F, Prima G, Lailé D, Gordin DM, Thibon I, Ansel D. Synthesis and phase transformations of beta metastable Ti-based alloys containing biocompatible Ta, Mo and Fe beta-stabilizer elements. *Adv Eng Mater*. 2006;8–10:961–5.
37. Fusayama T, Katayori T, Nomoto S. Corrosion of gold and amalgam placed in contact with each other. *J Dent Res*. 1963;42:1183–97.
38. Kobayashi E, Wang TJ, Doi H, Yoneyama T, Hamanaka H. Mechanical properties and corrosion resistance of Ti-6Al-7Nb alloy dental castings. *J Mater Sci Mater Med*. 1998;9:567–74.
39. Cheng X, Roscoe SG. Corrosion behaviour of titanium in the presence of calcium phosphate and serum proteins. *Biomaterials*. 2005;26:7350–6.
40. Padilla N, Bronson A. Electrochemical characterization of albumin protein on Ti-6Al-4 V alloy immersed in a simulated plasma solution. *J Biomed Mater Res A*. 2007;81:531–43.
41. Raistrick ID, MacDonald JR, Francschetti DR. *Impedance Spectroscopy Emphasizing Solid Materials and Systems*. New York: Wiley; 1987.
42. Lavos-Valereto IC, Wolyneć S, Ramires I, Guastaldi AC, Costa I. Electrochemical impedance spectroscopy characterization of passive film formed on implant Ti6Al7Nb alloy in Hank's solution. *J Mater Sci Mater Med*. 2004;15:55–9.